

## ROLLER PRINTED mc-SI SOLAR CELLS WITH OPTIMIZED FILL FACTORS OF 78%

F. Huster, P. Fath, E. Bucher

University of Konstanz, Department of Physics, P.O.Box X916, D-78457 Konstanz, Germany

Phone: +49 (0) 7531 / 88-4469, Fax: -3395, E-mail: frank.huster@uni-konstanz.de

**ABSTRACT:** Roller printing is a thick-film finger metallization technique capable of achieving optical finger widths down to 25  $\mu\text{m}$  with an efficiency improvement potential of 0.7% abs. over screen printed solar cells. Unfortunately up to now most roller printed cells suffered from poor fill factors of 65% to 75% which are not caused by high line resistances. In this study the reasons for the low fill factors of roller printed cells are investigated and identified as poor contact resistances and as non linear shunts, which are probably local Schottky shunts due to finger breakage. Both problems could be solved by the application of a different Ag paste, a new firing profile and the selection of a rigid finger profile, leading to mean fill factors of 78%. The optimized finger profile with an optical width of 50-60  $\mu\text{m}$  represents the best compromise between stability and efficiency still providing an efficiency improvement (so far calculated) over screen printing of 3.5% rel. (0.5% abs.). Within this study a cell efficiency of 15.7% on 10x10  $\text{cm}^2$  mc-Si equipped with a 35  $\Omega/\text{sq}$  emitter and 15.9% with a selective emitter have been reached.

Keywords: Roller printing - 1: Contact - 2: Multi-crystalline Si - 3

### INTRODUCTION

Roller printing is a high-throughput metallization technique for the self-aligning fine line printing on mechanically textured solar cells. This high quality finger metallization has the potential to provide an efficiency gain over standard screen printing of up to 0.7% abs. [1,2]. But so far most roller printed cells suffered from low fill factors of 65% to 75%. Therefore this study deals with the fill factor optimization of roller printed cells, including the identification and elimination of the FF limiting problems. Investigations of the IV-characteristics of roller printed cells suggest two main reasons for the fill factor losses: (1) an increased series resistance due to a poor contact resistance, and (2) a detrimental transport process at the p/n-junction probably due to local grid-to-base contacts with a Schottky diode behavior. These local base contacts are supposed to stem from microcracks or breakage of the small finger ridges. The main part of this paper addresses this assumption on the basis of a diversified finger profile investigation.

#### *Organization of the paper*

First the preparation of roller printed cells and the variety of investigated finger profiles are presented. The next section deals with the contact resistance optimization. Then the first investigation tries to find a correlation between the fragility of the finger ridge and a FF deterioration induced by finger breakage. Based on these results an assessment of the different profiles regarding mechanical reliability is suggested. For comparison purposes a supplementary experiment is performed where the emitter is locally removed before metallization by mechanical grooving. The second investigation is meant to judge the efficiency potential of each finger profile. As a combination of the results of both investigations the optimized profile regarding reliability and efficiency potential is selected and analyzed. Finally the cell results of this study are presented.

### CELL PROCESS

The cell process is based on an industrial-like PECVD  $\text{Si}_x\text{N}_y$  firing through process with the replacement of the screen printing front side metallization by roller printing of the fingers and busbar dispensing: mechanical structuring (V-grooves and finger ridges), alkaline etch and wafer cleaning,  $\text{POCl}_3$  diffusion to 35  $\Omega/\text{sq}$ , P-glass etch, PECVD  $\text{Si}_x\text{N}_y$  deposition, finger roller printing (Ag), busbar dispensing (Ag), back side screen printing (Al), co-firing, parasitic p/n junction isolation (dicing), and tabbing. As material neighboring Baysix mc-Si wafers with a starting thickness of 330  $\mu\text{m}$  and a size of 10x10  $\text{cm}^2$  are used.

In the metallization step the finger ridges, which are roughly 50  $\mu\text{m}$  protruding out of the V-textured front side, are coated with Ag paste by an even wheel<sup>1</sup>.

### FINGER PROFILES AND PROPERTIES

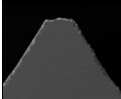
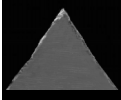
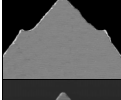
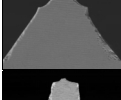
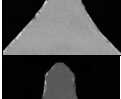
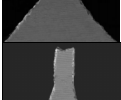
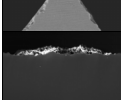

Using a beveled single blade with 70° tip angle on a dicing saw a variety of profiles for roller printing finger ridges are prepared. This structuring was based on the following design rules: the profile should be feasible to be structured by a wheel in the future, it should exhibit a high ratio of optical width to contact width and cross-section, and the different profiles should comprise fragile as well as rigid types. For each profile four cells are processed. The profiles and the properties of their respective metallized fingers, which are extracted from optical and scanning electron microscope images and line resistance measurements, are shown in Table I. The finger spacing is 1.5 mm except for type C (2 mm). Despite the fact that the properties of the metallized fingers depend not only on the profile of the finger ridge but also on the printing step (paste rheology, number of printing steps etc.), they are

---

<sup>1</sup> For further details on the roller printing technology see [1,2].

nevertheless representative for each profile and therefore used in the section “efficiency potential of the fingers”.

**Table I:** Description of investigated finger profiles and properties of metallized fingers (optical width, contact width and line resistance).

| SEM image width: 150 $\mu\text{m}$                                                  | Type / Description                      |                           | Width              |                     | Line                            |
|-------------------------------------------------------------------------------------|-----------------------------------------|---------------------------|--------------------|---------------------|---------------------------------|
|                                                                                     |                                         |                           | Opt. $\mu\text{m}$ | Cont. $\mu\text{m}$ | res. $\text{m}\Omega/\text{cm}$ |
|                                                                                     | RP: roller printing, SP: screen printed |                           |                    |                     |                                 |
|    | RP A                                    | rigid triangular          | 75                 | 120                 | 400                             |
|    | RP B                                    | simple triangular         | 60                 | 90                  | 900                             |
|    | RP C                                    | triangular, "pockets"     | 85                 | 140                 | 400                             |
|    | RP D                                    | triangular, small pockets | 80                 | 130                 | 350                             |
|   | RP E                                    | rigid fin                 | 50                 | 110                 | 350                             |
|  | RP F                                    | rigid fin, beveled edges  | 40                 | 100                 | 700                             |
|  | RP G                                    | fragile fin               | 30                 | 90                  | 700                             |
|  | SP                                      | for comparison            | 120                | 120                 | 400                             |

## CONTACT RESISTANCE OPTIMIZATION

Contact resistance measurements on roller printed solar cells published earlier [2] exhibited 10 to 30  $\text{m}\Omega\text{cm}^2$ . The application of a different Ag paste (also commercially available) and fine tuning of the firing conditions lead to reproducibly low contact resistances of 2 - 5  $\text{m}\Omega\text{cm}^2$ , which is frequently considered as a lower limit for thick-film contacts.

## FRAGILITY OF THE FINGER RIDGES

The exposed finger ridges are potentially prone to mechanical damage during processing. A damaged emitter due to finger breakage or microcracks underneath the finger grid generally leads to some kind of shunting. It is the purpose of this section to investigate the shunting and to find a correlation to the finger profile design.

### IV-measurements

While well-behaved solar cells can be described by a two-diode-model, “problematic” cells tend to differ from this simple behavior. Under the assumption that the diode currents  $J_{01}$  and  $J_{02}$  (representing the recombination processes in emitter&bulk and space charge region, resp.) are not significantly affected by the finger profile and by possible local shunts these currents are taken to be same for all roller printed cells made out of neighboring wafers.

From illuminated and  $J_{sc}$ - $V_{oc}$  IV-measurements the linear shunt resistance (from reverse bias) and the series resistance for each cell have been extracted. Finally the “ideal” dark IV-curve of each cell is reconstructed using these parameters in a two-diode-model. The differences between this modeled curve and the measured dark IV-curve is known as a hump and can be attributed to a non-linear shunt. Examples for humps are shown in figures 1 to 3 with modeled and measured dark IV-curves of roller printed cells.

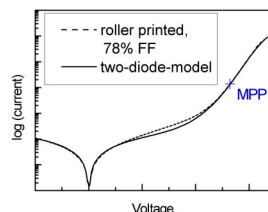


**Figure 1:** IV-curve with a negligible hump, typical for cells of type A, E and F (and also for screen printed cells).

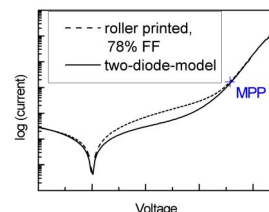
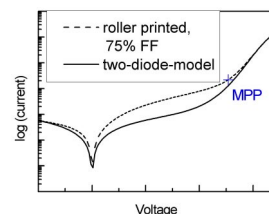


**Figure 2:** IV-curve with a medium hump, typical for cells of type C and D.



**Figures 1-3:** Comparison of calculated and meas. dark IV-curves. The medium hump indicates some Schottky shunts, but causes no FF deterioration. The extended hump in fig. 3 is affecting the FF, but not yet  $V_{oc}$ .

**Figure 3:** IV-curve with an extended hump, typical for cells of type G (and some of type B).

A similar observation is known from the breakage of pyramids on textured mono-crystalline silicon [3] and from edge recombination [4]. For the roller printed cells we assume that local grid-to-base contacts of the Ag-paste lead to small Schottky shunt contacts. In reverse bias these contacts have no effect due to their diode behavior. Applying a small forward voltage one can see a strong current increase and an asymmetrical IV-characteristic around  $V=0$ , which is normally symmetrical and governed by a linear shunt. With increasing voltage the additional Schottky current is limited by the base spreading resistance of the local contacts and finally the IV-curve is dominated by the cell diode. This behavior can be modeled by a diode in series with a resistance [5].

The fragile profile type “G” shows a pronounced hump as it could be expected. Most cells of the triangular types (B,C,D) also exhibit a hump which is smaller, while the rigid types (A,E,F) as well as untextured screen printed cells can be described by the two-diode-model without hump.

### Fill factor analysis

The mean fill factors as well as the series and shunt resistances are listed in Table II. Additionally the fill factor losses which can be attributed to the Schottky shunts and also the calculated series resistances (based on measurements of sheet resistance, line resistance and contact resistance) are shown. The detrimental influence of the hump on the fill factor can be seen for types B and G; the humps of types C and D on the other side do not affect the maximum power point. From Table II no severe

decrease of the linear shunt correlated to IV-humps can be detected.

**Table II:** Mean fill factors and resistances.

| Front contact   | FF meas | FF-loss by hump | R <sub>series</sub> meas. | R <sub>series</sub> calc. | Linear R <sub>shunt</sub> |
|-----------------|---------|-----------------|---------------------------|---------------------------|---------------------------|
|                 | %       | %               | Ωcm <sup>2</sup>          | Ωcm <sup>2</sup>          | Ωcm <sup>2</sup>          |
| RP type A, E, F | 77.9    | < 1%            | 0.37                      | 0.32                      | 2300                      |
| RP type B       | 74.6    | 2.7 %           | 0.60                      | 0.37                      | 3000                      |
| RP type C, D    | 78.1    | < 1 %           | 0.39                      | 0.32                      | 2900                      |
| RP type G       | 75.4    | 2.9%            | 0.39                      | 0.37                      | 1800                      |
| SP untext.      | 79.1    | < 1%            | 0.35                      | 0.44                      | 3600                      |

*Profile assessment*

The profile types B and G show significantly lower fill factors that can not be explained by series or linear shunt resistances. The shape of the IV-curves suggests that some finger breakage is indeed occurring for these profiles. But also for the other pointed triangular profiles C and D finger breakage must be assumed because of the occurrence of small humps. The rigid profiles A, E, and F on the other side seem to withstand the stresses typically caused by the handling in a pilot line environment.

**Table III:** Profile assessment regarding fragility.

| Type    | Description              | Qualification |
|---------|--------------------------|---------------|
| G       | fragile fin              | unqualified   |
| B       | simple triangular        | unqualified   |
| C, D    | other pointed triangular | problematic   |
| A, E, F | rigid triangular and fin | qualified     |

*Supplementary experiment*

By grinding grooves with a narrow dicing blade (30 μm) through the finger ridges after the Si<sub>x</sub>N<sub>y</sub> deposition and before the roller printing the emitter is damaged in well controlled manner. For this investigation the rigid profile type A has been chosen. The application of 3 and 17 cuts per wafer leads to 200 and 1100, resp., small contacts (contact area approx. 0.005 mm<sup>2</sup>) of the grid to the p-doped basis. Unfortunately some of the fingers do not bridge the gaps cut into the ridges and therefore the cells exhibit an increased series resistance. Nevertheless an IV-characteristic with a hump similar to that of roller printed cells with fragile finger profiles can be observed. The cells with 200 Schottky contacts have a FF of 74% and the ones with 1100 contacts 61%, but still maintain a linear shunt resistance of about 1000 Ωcm<sup>2</sup>.

**EFFICIENCY POTENTIAL OF THE FINGERS**

A common feature of roller printed fingers on protruding ridges is the improved ratio of the contact width and the cross-section to the optical width compared to screen printed fingers, leading to some efficiency gain. For each set of finger properties that determine the quality of the contact grid (optical width, contact width, line resistance) a certain optimal finger spacing exists. To exclude influences from Schottky shunts, non-optimized finger spacing, and differing contact resistances the comparison of the different finger profiles is better done by

calculating the cell efficiency instead of looking at cell parameters. This calculation is again using the two-diode-model, taking as variable input parameters the measured finger properties listed in Table I. The calculation is carried out for a V-textured front side and different emitters and compares the cell efficiencies to that of a perfect front contact characterized by negligible finger shading and series resistance (of finger and emitter). For comparison also buried contact (BC, parallel or perpendicular to the V-grooves) and screen printing metallization are considered. The high performance screen or stencil printing refers to fingers with a cross-section of 80 μm x 20 μm.

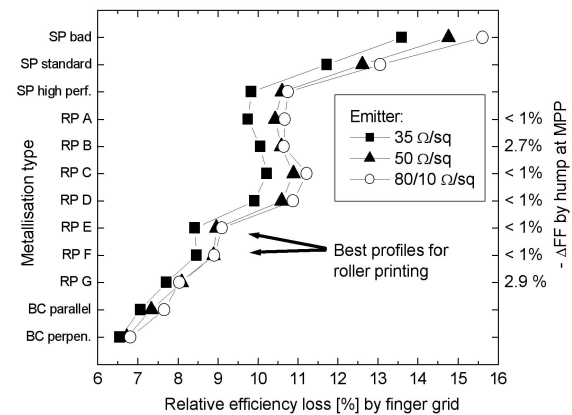


**Figure 4:** Calculated efficiency losses by different finger grids compared to a “perfect” front contact. On the right axes the observed FF-losses due to humps are displayed.

*Profile assessment*

Profiles A – D give an efficiency gain over standard screen printed fingers of only 2% relative. On the other side the high-end but fragile profile G (optical finger width 30 μm) approaches the efficiency performance of plated contacts. The rigid types E and F promise an efficiency gain of 3.5% relative over standard screen printing.

**OPTIMIZED FINGER PROFILE**

The optimal(um?) finger profile is a compromise between mechanical stability and efficiency improvement, which is best achieved by profiles E and F. Fig. 5 shows a metallized finger of type E with the following properties:

- optical width: 50 - 60 μm
- contact width: 110 μm
- cross-section: 950 μm<sup>2</sup> (line resistance 350 mΩ/cm)

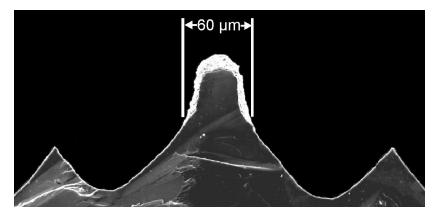


**Figure 5:** Typical view of the best finger profile (type E), roller printed and fired. An optical width of 40 – 50 μm on this type and dimension of finger ridge seems to be achievable by a further printing improvement.

**CELL RESULTS**

In Tables IV and V the mean and best cell results are shown. The cell efficiencies do not exactly reflect the

distribution that has been calculated in the previous section due to the reasons, which are also described there. Additionally some cells have been processed with a selective emitter.<sup>2</sup>

**Table IV:** Cell results (mean values, 35 Ω/sq)

| Type (number of cells) | FF [%] | $J_{sc}$ [mA/cm <sup>2</sup> ] | $V_{oc}$ [mV] | $\eta$ [%]  |
|------------------------|--------|--------------------------------|---------------|-------------|
| RP A (4)               | 78.6   | 32.4                           | 609           | <b>15.5</b> |
| RP B (4)               | 74.6   | 32.8                           | 610           | <b>14.9</b> |
| RP C (4)               | 77.9   | 32.5                           | 611           | <b>15.5</b> |
| RP D (4)               | 78.2   | 32.2                           | 610           | <b>15.3</b> |
| RP E (2)               | 78.4   | 32.4                           | 612           | <b>15.5</b> |
| RP F (3)               | 77.1   | 33.1                           | 611           | <b>15.6</b> |
| RP G (3)               | 75.4   | 32.7                           | 608           | <b>15.0</b> |
| SP untext. (10)        | 79.1   | 30.2                           | 616           | <b>14.7</b> |

**Table V:** Cell results (best cells)

| Type                     | FF [%] | $J_{sc}$ [mA/cm <sup>2</sup> ] | $V_{oc}$ [mV] | $\eta$ [%]  |
|--------------------------|--------|--------------------------------|---------------|-------------|
| RP F 35 Ω/sq             | 77.9   | 33.0                           | 609           | <b>15.7</b> |
| RP D sel. Em. 75/10 Ω/sq | 77.8   | 33.1                           | 616           | <b>15.9</b> |
| SP untext. 35 Ω/sq       | 79.9   | 30.7                           | 619           | <b>15.2</b> |

## CONCLUSIONS

In this study the reasons for the low fill factors of roller printed cells have been identified as poor contact resistances and as non-linear shunts. These shunts are probably local Schottky contacts due to finger breakage, which is suggested by a hump in the IV-characteristics and the correlation of this hump to the fragility of the finger profiles. By the application of a different Ag paste, a new firing profile and the selection of a rigid finger profile, mean fill factors of 78% could be reached. The investigations on the fragility and on the efficiency potential of the different finger profiles helped to determine an optimized finger profile representing the best compromise between stability and efficiency. This finger profile has an optical width of 50 – 60 μm and provides an efficiency improvement (so far calculated) over screen printing of 3.5% rel. (0.5% abs.). Within this study a cell efficiency of 15.7% on 10x10 cm<sup>2</sup> mc-Si equipped with a 35 Ω/sq emitter and 15.9% with a selective emitter have been reached.

## OUTLOOK

It is planned to verify the results using a larger number of cells but only four different profiles (like A, B, E, and G) with individually optimized finger spacing, thereby hoping to confirm the presented efficiency calculations by

experimental data. With type E as a new standard profile efforts will be made to push the cell efficiency above 16.5 %. The investigations on local Schottky shunts will be continued.

## ACKNOWLEDGEMENTS

The founding for development and research by the EU within the ASCEMUS project, contract number JOR3-CT98-0226, and HIT project under contract number JOR3-CT98-0223 as well as by the German BMWi under research grant 0329794 is gratefully acknowledged.

## REFERENCES

- [1] F. Huster, M. Spiegel, P. Fath, and E. Bucher, "Progress of the roller printing metallization technique towards an industrially compatible alternative to screen printing", *Proc. 16<sup>th</sup> EC PVSEC*, Glasgow, 2000, p. 1385
- [2] F. Huster, C. Gerhards, M. Spiegel, P. Fath, and E. Bucher, "Roller printed multicrystalline silicon solar cells with 16% efficiency and 25 μm finger width", *Proc. 27<sup>th</sup> IEEE PVSC*, Anchorage, 2000, p. 205
- [3] F. Hernando, R. Gutierrez, G. Bueno, F. Recart, V. Rodriguez, "Humps, a surface damage explanation", *Proc. 2<sup>nd</sup> WC PVSEC*, Vienna, 1998, p. 1321
- [4] Keith R. McIntosh and Christiana B. Honsberg, "The influence of edge recombination on a solar cell's I-V curve", *Proc. 16<sup>th</sup> EC PVSEC*, Glasgow, 2000, p. 1651
- [5] Matthew Stocks and Daniel Macdonald, "Non-ideal resistive effects in silicon solar cells", *Proc. 16<sup>th</sup> EC PVSEC*, Glasgow, 2000, p. 1671

<sup>2</sup> The modified process sequence consists of process steps mechanical finger structuring, alkaline etch, deep diffusion, P-glass etch, PECVD Si<sub>3</sub>N<sub>4</sub> masking, V-texturing, alkaline etch, shallow diffusion, metallization, firing, junction isolation, and tabbing.